Available online at www.sciencedirect.com
ScienceDirect
Solid-State Electronics 50 (2006) 1400–1405
SOLID-STATE ELECTRONICS
www.elsevier.com/locate/sse

Rapid and precise calculations of energy and particle flux for detailed-balance photovoltaic applications

Michael Y. Levy *, Christiana Honsberg

Department of Electrical and Computer Engineering, 140 Evans Hall, Newark, Delaware 19716-3130, USA

Received 8 February 2006; received in revised form 26 June 2006; accepted 30 June 2006

The review of this paper was arranged by Prof. Y. Arakawa

Abstract

The central problem that this paper addresses is the rapid and precise calculation of the energy and particle flux for detailed-balance photovoltaic applications. The calculation of energy and particle flux is essential to modeling the efficiencies and efficiency limits of solar energy conversion devices. Computing flux with the canonical Bose–Einstein integral is time consuming and, without due care, prone to error. The approach given herein, transforms the Bose–Einstein integral into a linear combination of incomplete Riemann zeta integrals. The numerical package that implements this method is benchmarked for precision by a number of means. These include comparisons between the Riemann zeta functions, and previously recorded values of solar cell limiting efficiencies from the literature. The rapidity of the numerical package is gauged by comparing the duration of flux calculations to other calculation methods.

Keywords: Solar cell; Photovoltaic; Detailed-balance; Flux; Bose–Einstein; Riemann zeta

1. Introduction

The calculation of energy and particle flux is essential to modeling the conversion efficiencies of solar energy converters, in general, and the efficiency limits of the converters, in particular. Such calculations are made when modeling the conversion efficiencies of various devices, such as photovoltaic converters [1], thermophotovoltaic devices [2], and multi-band solar cells [3]; as well as photovoltaic devices incorporating up-conversion [4] and down-conversion mechanisms [5]. Though efficiency limit modeling has been undertaken for decades [6], some of the advanced photovoltaic concepts that have arisen have stimulated the present day demand for higher performance methods to calculate flux. For example, determining the efficiency of devices with internally biased operating points, (e.g. intermediate band solar cell (IBSC) [3], serial-connected tandem [7], up-converter [4] and down-converter [5]) require many calculations just to determine the operating points, and hence are very time intensive. Further bolstering the demand for higher performance methods, are applications where it is necessary to calculate the flux when the chemical potential of the photons is very near to the band-gap of the converter. In such cases, the calculation of flux requires the evaluation near a singularity (cf. Eq. (1), which has a singularity as μ approaches E_A). A high performance method for calculating flux is obtained by transforming the canonical forms of the flux into a linear combination of integrals, whose integrands are functions of a single dummy variable. Look-up-tables (LUT) may then be computed over the domain of the dummy variable.

Flux is written canonically as a Bose–Einstein integral, which has no closed form solution. Therefore, some combination of numerical methods, expansions [8,9], and limiting expressions are required to evaluate flux. As regards numerical methods, numerically integrating the Bose–Einstein

* Corresponding author. Tel.: +1 302 831 0307.
E-mail addresses: mlevy@ece.gatech.edu, qb@UDel.edu (M.Y. Levy).

0038-1101/$ - see front matter © 2006 Elsevier Ltd. All rights reserved.
doi:10.1016/j.sse.2006.06.017

integral is time consuming and, without due care, prone to error. The errors largely derive from the limited degree of accuracy of numerical integration routines and the high order interpolation needed to fit the spectrum of the radiation. When modeling the efficiency limits of devices with internal constraints, the speed of computation is placed at a premium and the use of the Bose–Einstein integral becomes unsatisfactory. For example, in modeling the efficiency limit of an IBSC, the net flux of photons from the conduction band reservoir to the intermediate band reservoir must first be set equal, or as near to equal as numerically possible, to the net flux of photons from the intermediate band reservoir to the valence band reservoir. Additionally, in situations where it is necessary to evaluate radiation flux whose chemical potential is very near to the absorption edge of the matter, numerical computation of the Bose–Einstein integrals becomes very slow and subject to large numerical errors because of the need to evaluate near a singularity.

The approach given herein, transforms the Bose–Einstein integral into a linear combination of incomplete Riemann zeta integrals (IRZI). The integrands of each of the IRZI are functions of a single dummy variable, x. For each IRZI two LUT are created: one denoting intervals by which a composite integration is pre-computed across the numerical domain, $\mathscr{D}_x$, of the dummy variable x; and a second recording the computed values of the IRZI whose limits of integration are held by the first LUT. In those cases where calculating flux requires evaluating the Riemann zeta integrands for x outside of $\mathscr{D}_x$ limiting approximations to the integrands are employed; specifically, approximations where the component due to x outside of $\mathscr{D}_x$ are analytic. In those cases where calculating flux requires evaluating the Riemann zeta integrands for x inside of $\mathscr{D}_x$ the high-precision LUT are employed; such that over a large portion of the interval between the limits of integration, summation replaces numerical integration. The use of the limiting approximations and LUT allows for precise and rapid computation of flux.

The organization of the paper is as follows: Section 2 presents the details of this method, Section 3 shows the means by which the precision of the method has been verified, and Section 4 presents evidence that this method is, in most cases, faster than other methods.

2. Calculation of flux

To calculate flux rapidly and precisely an integral is sought such that its integrand is a function of a single dummy variable and its limits of integration allow it to be a proper definite integral. In order to avoid accruing numerical error, the limitations of the computer arithmetic must be considered with respect to the integrands. In regions where there is large floating-point error, appropriate limiting functions must be employed to approximate the integrands. Finally, consideration must be given to the generation of the LUT.

2.1. Form suitable for numerical computations

The integral describing photon flux, F_P, derives from the emissivity of the matter that the photons are interacting with, the density of photon modes, and the Bose–Einstein statistics. The canonical form of the flux is given as

$$F_P(E_A,E_B,T,\mu) = \begin{cases} \dfrac{2\pi}{c^2h^3}\displaystyle\int_{E_A}^{E_B} \dfrac{E^P\,dE}{\exp\left(\dfrac{E-\mu}{kT}\right)-1} & \text{if } \mu < E_A < E_B, \quad 0 < E_A < E_B, \\ 0, & \text{otherwise,} \end{cases} \tag{1}$$

where E_B and E_A are the upper and lower energy limits of the photon emission from the solid respectively, μ is the equilibrium chemical potential of the radiation, T is the surface temperature of the matter, c is the speed of light, h is Planck's constant, k is Boltzmann's constant and P takes the values 2 or 3 for the calculation of particle flux or energy flux respectively [1]. In future expressions for flux, it is understood that the inequalities given in Eq. (1) are satisfied so that that the flux is non-zero.

The first step in creating LUT, which expedite the rapidity and precision of flux calculations, is to transform equation (1) into a form whose integrands are functions of unitless, dummy variables. By the following substitution, $y = (E-\mu)/kT$, Eq. (1) is rewritten as a linear combination of IRZI:

$$F_P(E_A,E_B,T,\mu) = \sum_{p=1}^{P+1} a_{p-1} \int_{\frac{E_A-\mu}{kT}}^{\frac{E_B-\mu}{kT}} \frac{y^{p-1}\,dy}{\exp(y)-1}. \tag{2}$$

where a_{p-1} may be determined from carrying through the algebra. Though the integrands of Eq. (2) are a function of a unitless dummy variable, the form of Eq. (2) is not always suitable. Such is the case when the upper limit of the emissivity tends towards infinity, which is the case in the majority of detailed-balance efficiency calculations. In such circumstances, the forms given by Eqs. (1) and (2) become improper integrals. Thus, the numerical integration tends to become arbitrary, as the following question must be answered: Just how large is infinity? With some authors, for example, choosing 6 eV [10]. In order to surmount this problem the substitution $x = 1/y$ is employed and thus flux is re-written as

$$F_P(E_A,E_B,T,\mu) = \sum_{p=1}^{P+1} a_{p-1} \int_{\frac{kT}{E_B-\mu}}^{\frac{kT}{E_A-\mu}} \frac{dx}{x^{p+1}\left[\exp\left(\frac{1}{x}\right)-1\right]}. \tag{3}$$

The form of Eq. (3) is superior to the two previous forms because it allows for the construction of LUT and it avoids the difficulty of evaluating improper integrals. An additional benefit of Eqs. (2) and (3) is that the individual integrals (for p a positive integer greater than one) may be compared with closed form expressions of the Riemann zeta functions, thus allowing checks on the precision of the method.

2.2. Limitations of computer arithmetic

Computer arithmetic further complicates the precise computation of flux. When x is small, one must guard against underflow errors when evaluating the Riemann zeta integrands. For comparison, when E of Eq. (1) is large, one must guard both against underflow and round-off errors. Further, when x is large the floating-point error caused by the subtraction in the denominator causes the integrands to oscillate with x, until finally one-over-zero errors occur. This may be seen clearly by plotting the relative error between the integrands and a limiting approximation to the integrands. Fig. 1 illustrates for the case $p = 3$ that the Riemann integrand of Eq. (3) begins to oscillate with x but that the integrand may be approximated by a limiting expression given in Eq. (5). For comparison, when μ nears E_A, the same phenomenon is observed for the Bose–Einstein integrands. As shown in Fig. 2, when x increases a bit beyond 1×10^7, the relative error between the two integrands stops decreasing and begins to oscillate with larger and larger amplitude. Thus, for all the Riemann integrals, there is a fixed domain of x, $\mathscr{D}_x$, such that the integrands are both computable and stable. The limits of this domain largely depend upon the machine precision of the microprocessor, yet, some judgment is necessary as to the location of the upper cutoff of the domain. The authors have found that for a machine precision of order 1×10^{-16}, that $\mathscr{D}_x = [1.41 \times 10^3, 1.00 \times 10^7]$ is suitable for all the orders of the IRZI that are of interest ($p = 1, 2, 3, 4$). The limits of this numerical domain derive purely from the constraints of the computer arithmetic, as opposed to considerations regarding the spectrum of a given radiation of interest.

In those cases where there is a contribution to the flux from outside the boundaries of $\mathscr{D}_x$, limiting expressions must be used to calculate that contribution. The authors recommend the use of $\widehat{F}_P^{\text{low}}$ and $\widehat{F}_P^{\text{high}}$ to calculate that contribution if $kT/(E_B - \mu) < \min(\mathscr{D}_x)$ and if $kT/(E_A - \mu) > \max(\mathscr{D}_x)$ respectively, where:

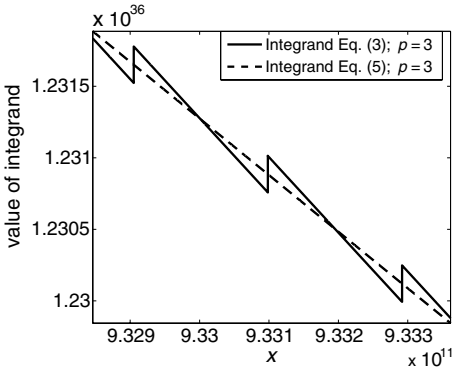

Fig. 1. For large x, evaluation of Riemann zeta integrands is subject to round-off errors that are caused by the denominator terms. In these cases, the integrands may be approximated by limiting functions such as those given in Eq. (5). This figure shows the integrand of Eq. (2), $(x^{p+1}[\exp(1/x) - 1])^{-1}$, and that of Eq. (5), x^{-p}, for the case $p = 3$.

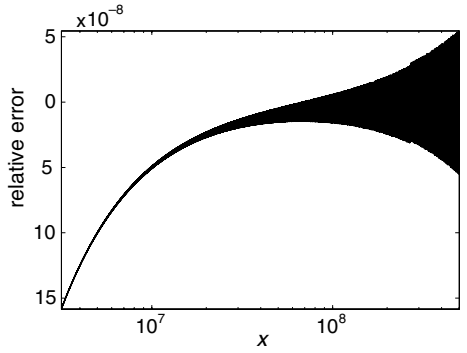

Fig. 2. As x increases beyond 1×10^7, the relative error between the integrands of Eqs. (3) and (5) begins to oscillate with increasing amplitude. This is true for $p = 1, 2, 3, 4$. This figure shows $p = 3$.

$$\widehat{F}_P^{\text{low}}(E_A, E_B, T, \mu) = \sum_{p=1}^{P+1} a_{p-1} \int_{\frac{kT}{E_B - \mu}}^{\min(\mathscr{D}_x)} \frac{dx}{x^{p+1} \exp\left(\frac{1}{x}\right)}. \tag{4}$$

$$\widehat{F}_P^{\text{high}}(E_A, E_B, T, \mu) = \sum_{p=1}^{P+1} a_{p-1} \int_{\max(\mathscr{D}_x)}^{\frac{kT}{E_A - \mu}} \frac{dx}{x^p}. \tag{5}$$

Note that Eqs. (4) and (5) are both analytic and thus can be expressed in a closed-form, which further augments both the precision and the speed of computation, as numerical integration is unnecessary. In addition to their utility in approximating flux outside the bounds of $\mathscr{D}_x$, Eqs. (4) and (5) may be used to gauge the accuracy of computations while debugging software, and even, in some cases, to approximate the flux across the whole limit of integration, E_A to E_B, as will be seen in Section 3.

2.3. Look-up-tables for Riemann zeta integrals

Each of the Riemann integrals is associated with two LUT: one containing increasing values of x, beginning with $\min(\mathscr{D}_x)$ and ending with $\max(\mathscr{D}_x)$; and a second recording the computed values of the IRZI between two successive entries in the first LUT. For example, in calculating the particle flux in a situation such that $\min(\mathscr{D}_x) < E_A < E_B < \max(\mathscr{D}_x)$, the operations given in Eq. (6) are performed, where $x_n^{(p)}$ is the smallest value in the first LUT associated with the pth Riemann zeta integral greater than $kT/(E_B - \mu)$, $x_N^{(p)}$ is the largest value in the first LUT associated with the pth Riemann zeta integral less than $kT/(E_A - \mu)$, and all the integrals in the inner summation are pre-computed and recorded in the second LUT associated with the pth Riemann zeta integral.

$$F_P(E_A, E_B, T, \mu) = \sum_{p=1}^{P+1} a_{p-1} \left(\int_{x_N^{(p)}}^{\frac{kT}{E_A - \mu}} \frac{dx}{x^{p+1}\left[\exp\left(\frac{1}{x}\right) - 1\right]} + \sum_{m=n}^{N-1} \int_{x_m^{(p)}}^{x_{m+1}^{(p)}} \frac{dx}{x^{p+1}\left[\exp\left(\frac{1}{x}\right) - 1\right]} + \int_{\frac{kT}{E_B - \mu}}^{x_n^{(p)}} \frac{dx}{x^{p+1}\left[\exp\left(\frac{1}{x}\right) - 1\right]} \right). \tag{6}$$

For the special case where $n = 1$, the last integral in Eq. (6) is approximated by the limiting expression given in Eq. (4). Similarly, for the special case where $x_N = \max(\mathscr{D}_x)$, the first integral in Eq. (6) is approximated by the limiting expression given in Eq. (5).

Pre-computing LUT in the manner of Eq. (6) not only speeds up calculations during run time, but, in general provides more precise results. The reason being is that numerical integration routines are almost exclusively based upon interpolation polynomials and the integrands of the Riemann zeta integrals must be interpolated with polynomials of very large order. Thus, in general, numerical integration routines will have a difficult time maintaining both precision and rapidity, especially over large intervals [11]. Therefore, the method that the authors adopt is to generate LUT by composite integration across $\mathscr{D}_x$.

In performing the composite integrations, the authors first perform *B*-form least-squares spline approximations of order six to the integrand functions using MATLAB's spap2 function. The spline approximations are performed by logarithmically sampling the integrand functions five thousand times. Next, MATLAB's newknt function is employed to choose a knot sequence that divides the numerical range into five intervals. The knot sequence obtained by this procedure is shown in Fig. 3 for the case $p = 2$. Next, each interval is logarithmically partitioned into sub-intervals. The number of sub-intervals in a given interval is increased until the integral across the interval converges. Table 1 gives the intervals' breakpoints for the cases $p = 1, 2, 3$, and 4. For each of these, to obtain convergence, the first interval (small x) is broken into 80 sub-intervals, the last interval is broken into 600 sub-intervals, and the remaining three intervals are broken into 10 sub-intervals.

The next section provides evidence that the method developed in this section has a high degree of precision.

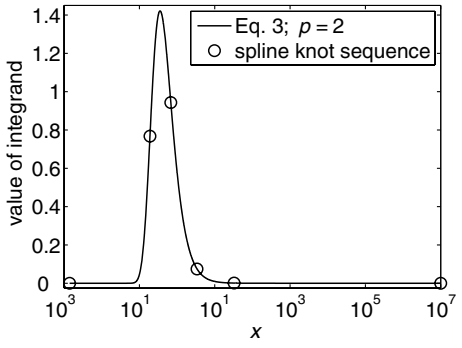

Fig. 3. Integrand of the Riemann zeta integral of order two within the numerical domain $\mathscr{D}_x$. The circles indicate the interval demarcations as obtained by the spline approximation.

Table 1
The value of x that demarcates the ith breakpoint of the integrand of the pth IRZI

i	$p = 1$	$p = 2$	$p = 3$	$p = 4$
1	1.4×10^{-3}	1.4×10^{-3}	1.4×10^{-3}	1.4×10^{-3}
2	5.2×10^{-1}	1.9×10^{-1}	1.3×10^{-1}	1.1×10^{-1}
3	6.7×10^{0}	6.8×10^{-1}	3.6×10^{-1}	2.4×10^{-1}
4	1.9×10^{2}	3.4×10^{0}	1.2×10^{0}	6.5×10^{-1}
5	3.8×10^{4}	3.3×10^{1}	5.4×10^{0}	2.2×10^{0}
6	1.0×10^{7}	1.0×10^{7}	1.0×10^{7}	1.0×10^{7}

These demarcations are obtained by a spline approximation to the integrands.

3. Verification of high-precision

The numerical software that implements this method is benchmarked for precision by a number of means. These include comparisons between the Riemann zeta functions, and previously recorded values for solar cell limiting efficiencies from the literature.

Most importantly, the fact that the complete Riemann zeta integrals for positive integers greater than one are given in closed form allows for a comparison that provides conclusive indication of the precision of the combination of LUT and limiting expressions. For $p = 2, 3, 4$ the simulator showed an absolute error of order 1×10^{-14} such that the computed value was greater than the closed form expression. The computational package is also benchmarked against a number of efficiency limit results for the single p–n junction solar cell and the IBSC.

In order to further judge the precision of the numerical package, results are compared with previous results obtained by the literature. Under maximum solar concentration, a solar surface temperature, T_s, of 5762 K, and a planetary surface temperature, T_p of 288 K, the efficiency limit of the single junction solar cell (SJSC) is calculated as 40.7% when the lower limit of the emissivity, which is equal to the band-gap E_g, is 1.06 eV and the upper limit of the emissivity tends towards infinity. This compares favorably to the results of De Vos (40.8% for $E_g = 1.15$ eV) [1]. It is worth noting that under these conditions if Eq. (4) is used to approximate the solar cell flux over the complete limit of integration, $x = [0, k \times T_s/E_g]$ (where $\mu = E_g \times (1 - T_p/T_s)$ [1]), which is justified because for $E_g = E_A$ of order 1 eV the integrand of Eq. (3) is dominated by the exponential term, then the solar cell particle flux may be approximated analytically. The resultant value will be slightly larger than what would be obtained from numerical calculations using Eq. (3) because, for all values of x, the denominator of Eq. (4) is greater than the denominator of Eq. (3). Thus a ceiling is obtained, whereby any computed efficiency above this ceiling is patently invalid. The efficiency limit computed in this manner, for the identical conditions stated in the beginning of this paragraph, establishes a ceiling of 40.8%. Using the same temperatures as listed above, but with a solar concentration of 1×, the optimum efficiency is computed as 31.0% when $E_g = 1.26$ eV. These results compare favorably with the work of De Vos, who records the identical efficiency when $E_g = 1.30$ eV [1]. The numerical package is also benchmarked on the efficiency limit of a SJSC at full concentration but with

$T_s = 5759$ K and $T_p = 300$ K. The results of such calculations provide an efficiency limit of 40.6% at $E_g = 1.06$ eV, which compares favorably to the previously reported result under identical conditions: 40.7% at $E_g = 1.06$ eV [12].

Finally, the software package is benchmarked against previous calculations of the IBSC. The numerical software obtains a conversion efficiency of 63.2%, which is obtained when the effective band-gap between the conduction band and valence band is 1.95 eV and the band-gap between the intermediate band and valence band is 0.71 eV. This result compares exactly with the efficiency limit as defined here [3]. Additionally, under 1-sun illumination the simulator calculates an optimum efficiency of 46.8%, which is obtained when the effective band-gap between the conduction band and valence band is 2.40 eV and the effective band-gap between the intermediate band and valence band is 0.92 eV. This result again compares favorably with the previously reported optimized efficiency of 46.0%, which is reported to occur when the effective band-gap between the conduction band and valence band is 2.43 eV and the effective band-gap between the intermediate band and valence band is 0.93 eV [10].

The next section presents a verification of the rapidity of the method formulated herein.

4. Verification of rapidity

In order to gauge the rapidity of the method, it must be compared to other methods of calculating flux. The method is benchmarked by comparing the average durations of flux calculations as per the expressions given by Eqs. (1)–(3), and Eq. (3)*; where Eq. (3)* signifies the use of Eq. (3) with the incorporation of the LUT as well as the limiting functions given in Eqs. (4) and (5). Table 2 shows how these different methods of calculation compare for twelve unique cases, all of which are performed with a numerical tolerance of 1×10^{-14}. These specific cases are chosen because they are typical for detailed-balance applications with internally biased operating points and applications with multiple absorbers. In order to minimize the temporal variability with respect to the evaluation of the twelve cases, for each case, the duration is given as the average of 500 identical calculations.

The data of Table 2, which is obtained with a 3.6 GHz processor, indicates that for nine of the twelve cases, the method that is developed herein is roughly between five times and a hundred times faster than the next fastest method. The gains in speed tend to increase as the value of μ approaches its asymptote E_A. Under most circumstances, the method developed herein requires that a numerical integration routine be called $2 \times (P + 1)$ times; which is compared to a single call if using the Bose–Einstein integral of Eq. (1). However, the duration is never three times slower as compared to the calculations using Eq. (1); further, in only two of the twelve cases is the method developed herein more than three times slower than the fastest method. Yet, in applications that require the determination of the internally-biased operating points, many more flux calculations must be made for μ greater than zero as compared with only a small number of flux calculations where μ is equal to zero. Therefore, for these detailed-balance applications, significant time saving may be achieved by the adoption of the method presented herein.

Table 2
Average duration of 500 identical flux computations for 12 unique input conditions, each of which are computed by four different methods

$F_P(E_A, E_B, T, \mu)$	Average duration of calculation (ms)			
	Eq. (1)	Eq. (2)	Eq. (3)	Eq. (3)*
$F_2(0.7, 1.2, 6000, 0)$	540	130	190	63
$F_2(1.2, 2.0, 6000, 0)$	710	180	180	51
$F_2(2.0, 6.0, 6000, 0)$	1700	410	310	46
$F_2(0.7, 1.2, 300, 0)$	1700	16	15	29
$F_2(1.2, 2.0, 300, 0)$	1700	10	10	29
$F_2(2.0, 6.0, 300, 0)$	15	10	10	29
$F_2(0.7, 1.2, 300, 0.6)$	1800	570	400	41
$F_2(1.2, 2.0, 300, 1.1)$	1800	560	430	41
$F_2(2.0, 6.0, 300, 1.8)$	1800	320	220	31
$F_2(0.7, 1.2, 300, 0.7 \times (1 - 10^{-9}))$	1900	2100	3600	25
$F_2(1.2, 2.0, 300, 1.2 \times (1 - 10^{-9}))$	1900	2100	3600	25
$F_2(2.0, 6.0, 300, 2.0 \times (1 - 10^{-9}))$	1900	2200	3600	25

These conditions are selected because they are typical for detailed-balance efficiency calculations. The values of E_A, E_B and μ are given in electron Volts.

5. Conclusions

A method is formulated to rapidly and precisely calculate particle flux and energy flux for detailed-balance efficiency calculations. The method transforms the canonical Bose–Einstein integral into a linear combination of incomplete Riemann zeta integrals. By use of this transformation, look-up-tables are generated that record the results of precomputed composite integration. The precision of the method is established by comparing the numerically computed values of the Riemann zeta integrals with the closed-form expressions for these integrals. An absolute error of 1×10^{-14} is obtained between the two. The rapidity is gauged by comparing the duration of various flux calculations using several different methods. It is found that, under most circumstances, the formulated method is between five times and one hundred times faster than other methods.

Acknowledgements

M.Y.L. thanks Dr. A. Martí for providing details of his numerical package, Dr. E. Croot for his suggestion of the Bernoulli generator, and for other mathematical assistance, and G. Levy for his technical mantra "do it systematically". Both author give thanks to the U.S. National Renewable Energy Laboratory for their financial support through subcontract XAT-5-44277-01 administered by M. Symko-Davies and R. McConnell.

References

[1] De Vos A. Endoreversible thermodynamics of solar energy conversion. Oxford University Press; 1992, p. 96, 99, 120.
[2] Badescu V. Upper bounds for solar thermophotovoltaic efficiency. Renew Energy 2005;30:211–25.
[3] Luque A, Martí A. Increasing the efficiency of ideal solar cells by photon induced transitions at intermediate levels. Phys Rev Lett 1997;78:5014–7.
[4] Trupke T, Green MA, Würfel P. Improving solar cell efficiencies by up-conversion of sub-band-gap light. J Appl Phys 2002;92:4117–22.
[5] Trupke T, Green MA, Würfel P. Improving solar cell efficiencies by down-conversion of high-energy photons. J Appl Phys 2002;92:1668–74.
[6] Shockley W, Queisser H. Efficiency of p–n junction solar cells. J Appl Phys 1961;32:510–9.
[7] Brown AS, Green MA. Detailed balance limit for the series constrained two terminal tandem solar cell. Physica E 2002;14:96–100.
[8] Ng EW, Devine CJ, Tooper RF. Chebyshev polynomial expansion of Bose–Einstein functions of orders 1 to 10. Math Comput 1969;23:639–43.
[9] Ng EW, Devine CJ. On the computation of Debye functions of integer orders. Math Comput 1970;24:405–7.
[10] Luque A, Martí A. A metallic intermediate band high efficiency solar cell. Prog Photo 2001;9:73–86.
[11] Burden R, Douglas Faires J. Numerical analysis. 6th ed. Brooks/Cole Publishing Company; 1997, p. 199.
[12] G.L. Araújo, A. Martí, In: Proceedings of 11th EC PVSEC, Montreaux; 1992. p. 142–5.